

Original Article

Evaluation of Geometric Distortion Artifacts in Structural Magnetic Resonance Imaging

Sadegh Shurche¹, Nader Riyahi-Alam^{*2}

1- MSc Student, Physics and Medical Engineering Department, Medical Faculty, Tehran University of Medical Sciences, Tehran, Iran.

2- Professor, Physics and Medical Engineering Department, Medical Faculty, Tehran University of Medical Sciences, Tehran, Iran.

Received: 29 March 2017

Accepted: 13 May 2017

Key Words:

Magnetic Resonance Imaging,
Artifacts,
Phantom,
Reproducibility.

ABSTRACT

Purpose- Geometric errors in images, known as image distortion, are among the main problems in magnetic resonance imaging, including 3D imaging, measuring blood flow velocity, functional imaging and treatment planning in radiation therapy. The geometric distortion in MRI images is due to the non-uniformity of the magnetic field and nonlinearity of gradients. In the current study, the accuracy and the reproducibility of the images were respectively evaluated by phantom measuring and repeating the measurements in the phantom and then correcting these geometric errors.

Methods- The magnetic resonance imaging of the phantom was performed using a 3 Tesla Siemens Prisma MRI machine to measure the geometric distortion using the network pattern. Spin echo protocol was repeated three times with T_1 , T_2 and PD weightings to measure the reproducibility of image distortion. Image distortion was evaluated by measuring the distance between the edges using a MATLAB (version 8.3.0.532, MathWorks) program. Furthermore, the non-uniformity of the magnetic field and the nonlinearity of the gradients were examined using appropriate phantoms.

Result- The average error obtained in a 25 cm field of view was 1 pixel in both directions, x and y, (each pixel was 1.024 mm). Based on the phantom images, the device gradient was quite linear. Furthermore, considering the B_1 and B_0 fields' measurements, the B_0 of the device was measured 0.3125 ppm over a 24 cm DSV (Diameter Of Spherical Volume).

Conclusion- A minor brain coil displacement of 1 pixel will let the device be used in 3DMRI, velocity MRI, FMRI and RTTP.

1. Introduction

Currently, MRI devices are extensively used in advanced imaging centers to create high-resolution images and to show anatomical and pathological structures in the body. There are different parameters in MRI, which affect the final image. Therefore, creating a proper image of the organs or the veins is only possible by following appropriate imaging protocols and

determining the different correct parameters, such as FOV (Field of View), TR (Repetition Time), TE (Echo Time), ST (Slice Thickness) and FA (Flip Angle) [1]. Moreover, another key factor in creating an image is the good condition of different parts of the system. Furthermore, correct device functioning depends not only on the proper performance of the electronic circuits and different programs of the system, but also on the calibration

***Corresponding Author:**

Nader Riyahi-Alam, PhD

Physics and medical engineering Department, Medical Faculty, Tehran University of Medical Sciences, P.O.Box: 14176-13151, Tehran, Iran.

Tel: (+98)2166466383.

Email: riahialam@gmail.com

of each part of the system [2]. Calibration and performing quality control tests are essential in MRI systems [2]. Inspecting the different causes of image distortion in MRI systems, called artifacts, is of paramount importance. Hence, phantoms with definite shapes are provided in all imaging devices and are used in order to assure the correctness of the system [3,4]. The application of phantoms leads to diagnosing the deficiencies in the image compared to the original item [5]. One of the applications of the geometric distortion phantom is to control the quality of the systems. As shown in a study, 80% of the images produced by phantoms (in sagittal, axial and coronal cross-sections) agree with the used phantom's parameters [6]. The MRI image distortion identified by the phantom can be reduced using software programs [7]. In the present study, the rate of geometrical distortion in 3 Tesla MRI devices is inspected by designing and making a proper phantom.

2. Material and Methods

2.1. Selection of Concentration of Signalling Solution

The related studies and tests were carried out on a 3 Tesla Siemens Prisma MRI Scanner. Two series of solutions were used. One included CuSO_4 (10 and 20 mM), Magnevist (1:250) and distilled water and the other CuSO_4 (0.1, 0.3, 0.5 and 0.7 mM) and MnCl_2 (15, 20 and 25 mM). The solutions were tested carefully following proper imaging protocols. The solution type and its optimal concentration for filling the phantom were finally determined by drawing the curves of changes in the signal intensity against the TE and TR parameters and through making measurements. The Magnevist solution (1:250) was selected as the optimal solution among the two solutions that were prepared [8].

2.2. Fabrication of a Geometric Distortion Phantom

A fixed pattern is required to measure image distortion. To correct images, the proportionality between the constituents of MRI images must be considered and, then, some objects with known geometric shapes should be used to determine the degree of image distortion. This phantom

was designed employing AUTOCAD 2000. A Plexiglass block with density of 1.19 g/cm^3 and dimensions of $5 \times 20 \times 20 \text{ cm}$ was used. Using a 0.1 mm precision CNC lathe, a design in the shape of a crossword was cut on the surface of the block in the form of grooves, 40 mm deep and 2 mm thick with the distance of 10 mm between them. Inside, each groove was filled with the signal chain solution and a door was designed that could be closed and opened so that the solution could be replaced, and the inside of the grooves was washed to prevent contamination. The door was waterproofed using O-rings to prevent leakage from the solution inside the magnet bore or on the bed (Figure 1).

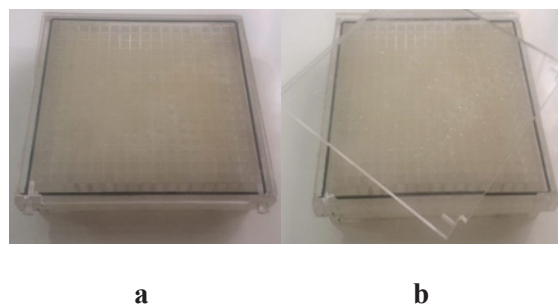


Figure 1. The geometric distortion phantom. A Plexiglass block with the density of 1.19 g/cm^3 and the dimensions of $5 \times 20 \times 20 \text{ cm}$ was used. a) Close. b) Open.

2.3. Fabrication of an Oil Phantom

To verify the uniformity of B_0 and B_1 fields, a cylindrical phantom, with a diameter of 24 cm and a height of 25.5 cm, was made of Plexiglass and filled with vegetable oil (Figure 2).



Figure 2. Cylindrical phantom to verify the uniformity of B_0 and B_1 . A cylindrical phantom, with a diameter of 24 cm and a height of 25.5 cm, was made of Plexiglass and filled with vegetable oil.

Table 1. Imaging parameters used for geometric distortion phantom in a 3 Tesla Siemens Prisma Model.

Protocole	S.T(mm)	TR(ms)	TE(ms)	FOV(cm)	Matrix Size
SE T ₁	5	500	19	25	256×200
SE T ₂	5	1000	103	25	256×200
SE PD	5	1000	19	25	256×200

2.4. Fabrication of Spatial Linearity Phantom

After fabricating the distortion phantom, the spatial linearity of the gradients was checked. This is an important factor in artifact development in images. First, a material as a contrast was needed to fill the spatial linearity phantom. A phantom was fabricated from Plexiglas with 250×250 mm dimensions, 50 millimeters thickness and 144 cavities (diameter :10 mm, depth: 50 mm, peritoneal spaces: 25 mm). Then, 144 glass tubes were made proportional to the dimensions of the cavities. The tubes were filled with CuSO₄ signalling solution with 10 mM concentration and were placed in the phantom cavities. The design accuracy was evaluated using CT images. The phantom of spatial linearity evaluation was fabricated through the above steps (Figure 3).

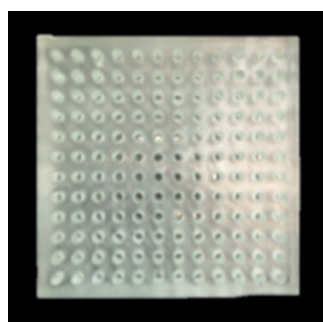


Figure 3. Spatial linearity phantom. A phantom was fabricated from Plexiglas with 250×250 mm dimensions, 50 millimeters thickness and 144 cavities (diameter:10 mm, depth:50 mm, peritoneal spaces: 25 mm).

2.5. Geometric Distortion Phantom Imaging

Image distortion in the Siemens Scanner was measured when the phantom was placed completely within the brain coil (Figures 5 and 6).

2.6. Oil Phantom Imaging

2.6.1. Uniformity of B₀

For measuring magnetic homogeneity, a uniform phantom was positioned in the center of the magnet and a GRE 3D pulse sequence was employed with TR=12 ms, flip angle=15 and two TE₁=4 ms and TE₂=8 ms.

2.6.2. Uniformity of B₁

For each study, six images with different flip angles of 50, 60, 80, 90, 100 and 120 were acquired with TR=1000 ms and TE=60 ms to investigate the capability of our method in determining the RF non-uniformity of the transmit and receiving head coil. To simulate non-uniform RF transmit and receive conditions, the head coil was used and the phantom was located partially outside the coil. With this configuration, six coronal sections of the phantom were acquired with the above mentioned flip angles.

2.7. Spatial Linearity Phantom Imaging

The phantom was placed on a lateral side to prepare cross-sectional images of the phantoms in order to achieve linearity of the gradients. Then, the central point lateral thickness of the phantom was adjusted using a laser beam. The location of the object was determined with a primary scan. A cross-section of the phantom from its centre was prepared. The phantom was prepared using Spin Echo (SE) protocol and cross-sectional imaging parameters (Table 2).

Table 2. Imaging parameters used for spatial linearity phantom in a 3Tesla Siemens Prisma Model.

TR	TE	Slise	ST	FOV
580 ms	9 ms	3	2 mm	20 cm

2.8. Analysis of Geometric Distortion Phantom Images

First, a transverse image was taken as the guiding image, and used to adjust the image. The difference between the observed dimensions and the actual ones is called geometric displacement. The following relation is used to calculate the geometric displacement or distortion of the image:

$$\frac{\text{Real Dimension}-\text{Observed Dimension}}{\text{Real Dimension}} \times 100 \quad (1)$$

The observed dimensions were obtained by measuring the distance between the edges in pixels (these dimensions are converted into mm considering the resolution of the image).

The reproducibility measurement of distortion was calculated by measuring the mean and standard deviations of the distortion and applying the following equations (1):

$$\text{Mean} = \sum_{i=1}^n \frac{D_i}{n} \quad (2)$$

$$\text{standard deviation} = \sqrt{\sum_{i=1}^n \frac{(D_i-\text{Mean})^2}{n-1}} \quad (3)$$

$$CV = \frac{\text{Standard Deviation}}{\text{Mean}} \quad (4)$$

where D_i is geometric error i and n is the number of geometric displacement measurement locations.

To measure the reproducibility of image distortion in the Siemens Scanner, the imaging was repeated three times in a single day without repositioning the phantom (CV_1), and again on three different days with repositioning the phantom (CV_2) in the x and y directions, when the phantom was completely placed within the brain coil. It is expected that the value of CV_1 will be less than five percent and less than that of CV_2 .

Then, we corrected the image error using the measurement results by IMAGEJ software (National Institutes of Health, USA) (Figure7).

2.9. Analysis of Uniformity of B_0 Images

For B_0 measurement, the difference in echo times of two GRE 3D sequences was 4 ms, which corresponds to 160 Hz per phase cycle, a phase shift

of 90 or one quarter of a cycle. It means that there is a 40 Hz difference in the resonance frequency. The magnetic field inhomogeneity is calculated as 40 Hz/128 MHz (the center frequency at 3 T) or 0.3125 ppm over a 24 cm DSF.

2.10. Analysis of Uniformity of B_1 Images

Various methods have been introduced for measuring transmitted B_1 and receiving sensitivity distributions of RF coils. We used a routine θ -180 Spin Echo pulse sequence. By varying the flip angle, six different images were acquired for each slice. The signal intensity was measured at different points. A mathematical model was fitted using the measured data by applying the relevant rotation matrices to the magnetization vector. Two functions, $T(r)$ and $R(r)$, were obtained as a result of the curve fitting process, which reflect the RF transmit and receive uniformity, respectively.

2.11. Analysis of Spatial Linearity Phantom Images

Figure 10 shows cavities in the phantom as bright spots in a dark context. No change in the location of the cavities around the phantom compared to other areas is the criterion for linearity evaluation in the image. In this case, the uniformity of RF pulse and the linearity of the gradients can be ensured.

Equation 1 can be used to determine the linearity in case of non-uniformity. For this purpose, the diameter of the tubes containing the signalling solution should be measured in the image and compared with the actual data.

Acceptable error rate in the nonlinearity of the image in a 25 cm field of view or greater than 25 cm is less than 5 %. Non-uniformity should be announced and resolved in an acceptable error rate $> 5\%$.

3. Results

3.1. Measuring the Reproducibility of Image Non-Uniformity

Table 3 and 4 show the results of measuring the reproducibility of image non-uniformity in the device in both directions of x and y .

Table 3. Results of measuring the reproducibility of image non-uniformity in the device in both directions of x and y.

Protocole	Percent of Distortion in x Axes (mean ±SD)(1)	Percent of Distortion in y Axes (mean±SD)(1)
SE T ₁	2.80 ± 2.01	2.02 ± 2.44
SE T ₂	2.30 ± 2.30	2.13 ± 1.44
SE PD	3 ± 2.44	2.43 ± 1.23

Table 4. Results of measuring the reproducibility of image non-uniformity in both directions of x and y.

Protocole	Percent of Distortion in x axes (mean ±SD)(2)	Percent of Distortion in y Axes (mean±SD)(2)
SE T ₁	2.07 ± 2	2.08 ± 2.40
SE T ₂	2.01 ± 2.07	2.30 ± 1.30
SE PD	3.02 ± 2.04	2.40 ± 1.10

As suggested by Figures 5 and 6, the error obtained for the device in both directions of x and y was 1 pixel (each pixel is equal to 1.024 mm).

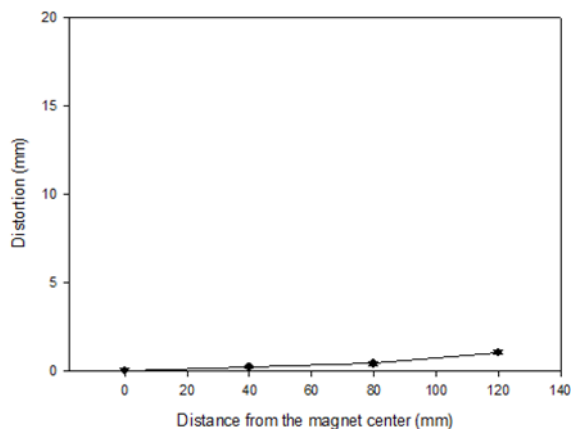


Figure 4. Graphs for non-uniformity of images at intervals of 0, 40, 80 and 120 mm from the center of the field.

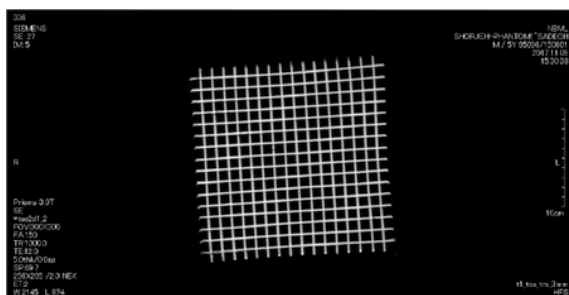


Figure 5. In the direction of y in the patient’s position, which indicates 1 pixel non-uniformity.

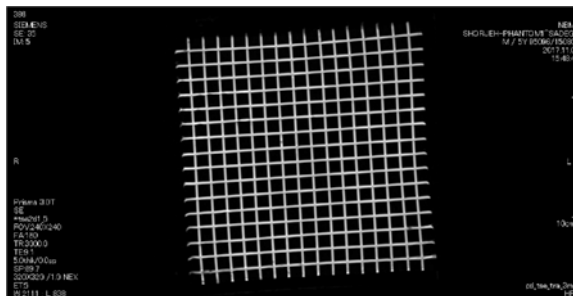


Figure 6. In the direction of x in the patient’s position, which indicates 1 pixel non-uniformity.

3.2. Geometric Distortion Correction

We corrected the image error using the measurement results by IMAGEJ software. (Figure 7).

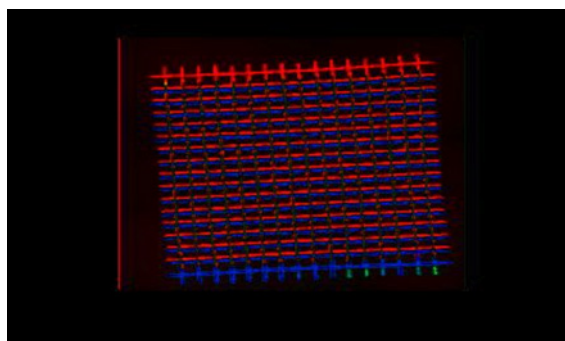


Figure 7. Phantom corrected image using IMAGEJ software. The red color of the image is corrupted and the blue color of the image has been corrected.

3.3. Uniformity of B₀ and B₁

RF waves were sent uniformly and the waves received by the head coil were uniform as well. The uniformity of B₀ field was equal to 0.3125 ppm over a 24 cm DSV (Diameter of Spherical Volume).

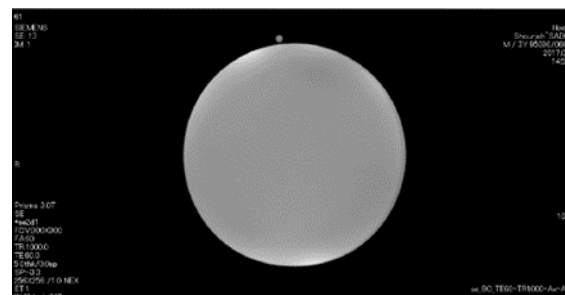


Figure 8. An image of the oil phantom acquired by head coil.

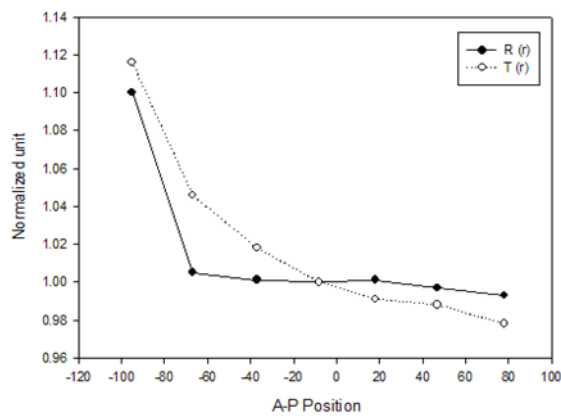


Figure 9. R(r) for head coil and T(r) for body coil of the system. Diagrams drawn using the method of Barker *et al.* [2].

3.4. Spatial Linearity of Gradient Coils

This image shows the linearity evaluation by phantom measurement with SE protocol (Figure 10). Nonlinearity cannot be detected due to a lack of changes in the size and shape of the tubes containing the signalling solution.

If the device gradient has a problem, correction functions can be estimated once and applied in post-processing on any acquisition type without changing the acquisition time [3].

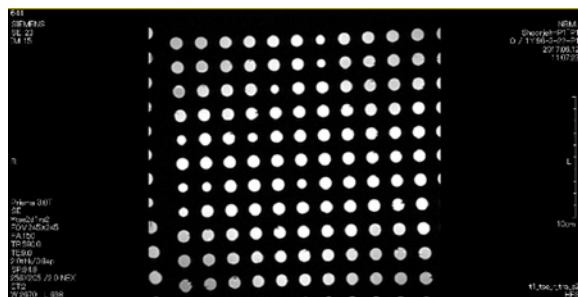


Figure 10. Image of spatial linearity phantom.

4. Discussion:

Our method for measuring transmitted B_1 and received sensitivity distributions of RF coils has some similarities to Barker's method [10], but, since it uses a $\theta=180$ spin echo, it is less sensitive to B_0 non-homogeneity. Also, when using this pulse sequence, we did not experience those slice profile problems reported by Barker *et al.*

We introduced a method that carefully examined

all parameters influencing geometric displacement. In measurements, the brain coil displacement was 1 pixel, hence, the device could be used in 3DMRI, velocity MRI, FMRI and RTTP. According to phantom studies, the observed displacement may be due to the uniformity of the magnetic field. Therefore, the proposed method can be used for quality control of different centers.

In the next steps, we will investigate the geometric error using a 3D phantom. Also, we aim to investigate geometric errors in the protocols of functional imaging.

Acknowledgments

We would like to thank the Food and Drug Administration (FDA) of the Islamic Republic of Iran and also the National Brain Mapping Lab (NMBL) for their contributions to this project.

References

- 1- Site of American College of Radiology Available: <https://www.acr.org>.
- 2- Chen C-C WY-L, Wai Y-Y, Liu H-L. Quality assurance of clinical MRI scanners using ACR MRI phantom: preliminary results. *Journal of digital imaging*, 17(4):279-84, 2004.
- 3- Price RR, Axel L, Morgan T, Newman R, Perman W, Schneiders N, et al. Quality assurance methods and phantoms for magnetic resonance imaging: report of AAPM nuclear magnetic resonance Task Group No. 1. *Medical physics*, 17(2):287-95, 1990.
- 4- Fellner C, Müller W, Georgi J, Taubenreuther U, Fellner FA, Kalender WA. A high-resolution phantom for MRI. *Magnetic resonance imaging*, 19(6):899-904, 2001.
- 5- Maris TG. Basic quality control in routine MRI. *Physica Medica*, 32:171, 2016.
- 6- Prott F HU, Willich N, Resch A, Stöber U, Pötter R. Comparison of imaging accuracy at different MRI units based on phantom measurements. *Radiotherapy and Oncology*, 37(3):221-4, 1995.
- 7- Mizowaki T NY, Okajima K, Kokubo M, Negoro Y, Araki N, et al. Reproducibility of geometric distortion in magnetic resonance imaging based on phantom studies. *Radiotherapy and Oncology*, 57(2):237-42, 2000.
- 8- Koh D-M, Collins DJ. Diffusion-weighted MRI in

the body: applications and challenges in oncology. *American Journal of Roentgenology*, 188(6):1622-35, 2007.

9- Mizowaki T, Nagata Y, Okajima K, Kokubo M, Negoro Y, Araki N, et al. Reproducibility of geometric distortion in magnetic resonance imaging based on phantom studies. *Radiotherapy and Oncology*, 57(2):237-42, 2000.

10- Barker G, Simmons A, Arridge S, Tofts P. A simple method for investigating the effects of non-uniformity of radiofrequency transmission and radiofrequency reception in MRI. *The British journal of radiology*, 71(841):59-67, 1998.

11- Langlois S, Desvignes M, Constans J-M, Revenu M. MRI geometric distortion: A simple approach to correcting the effects of non-linear gradient fields. *Journal of magnetic resonance imaging*, 9:821-31, 1999.